UNSUPERVISED GLOBAL IDENTIFICATION OF DIFFRACTIONS BASED ON LOCAL WAVEFRONT MEASUREMENTS

A. Bauer, B. Schwarz, T. Werner, and D. Gajewski

email: *alex.bauer@uni-hamburg.de*
keywords: *diffraction, wavefront, attribute, segmentation, zero-offset*

ABSTRACT

Multi-parameter stacking schemes like the common-reflection-surface (CRS) stack have shown to yield reliable results even for strongly noise-contaminated data. This is particularly useful for low-amplitude events such as diffractions, but also in passive seismic settings. As a by-product to a zero-offset section with a significantly improved signal-to-noise ratio, the CRS stack also extracts a set of physically meaningful wavefront attributes from the seismic data, which are a powerful tool for data analysis. Although the attributes vary laterally along the events, an analysis of their local similarity allows the global identification of measurements, which stem from the same diffractor or passive source, i.e., from the same region in the subsurface. In this work, we present a fully automatic scheme to globally identify and tag diffractions in simple and complex data by means of local attribute similarity. Due to the fact that wave propagation is a smooth process and due to the assumption of only local attribute similarity, this approach is not restricted to settings with moderate subsurface heterogeneity.

INTRODUCTION

In the recent years, seismic diffractions have gained increasing interest due to the fact that they are linked to complex geology nowadays often encountered in hydrocarbon exploration. However, they often have small amplitudes and thus are masked by high-amplitude events such as reflections. Local coherence analysis by means of multi-parameter stacking methods such as the common-reflection-surface stack (CRS, Jäger et al., 2001) not only significantly increases the signal-to-noise ratio, but also yields physically meaningful wavefront attributes, which may be utilized for further data analysis, such as time migration (Mann, 2002), diffraction separation (e.g. Dell and Gajewski, 2011; Schwarz and Gajewski, 2017), prestack data enhancement (Baykulov and Gajewski, 2009), prestack diffraction enhancement (Bauer et al., 2016), or velocity model building (Duveneck, 2004; Bauer et al., 2017b). In addition, the concept of wavefront attributes is equally applicable to passive seismic data (Schwarz et al., 2016; Diekmann et al., 2017) for which it allows simultaneous source localization and velocity inversion. In some of these methods, we aim to make use of the fact that all measurements that belong to the same diffraction are linked to the same spatial region in the subsurface. Whereas for time migration, prestack diffraction enhancement (Bauer et al., 2016) and diffraction separation (Dell and Gajewski, 2011) this knowledge may lead to better images, in the case of wavefront tomography for both active and passive data it provides an additional inversion constraint and even may allow the quantification of localization uncertainties (Bauer et al., 2017a). However, we can only make use of this feature if we are able to globally identify and tag diffractions in the data domain. In this work, we present a fully unsupervised scheme, which utilizes the local similarity of the zero-offset wavefront attributes obtained by the CRS stack for the global identification and tagging of diffractions.

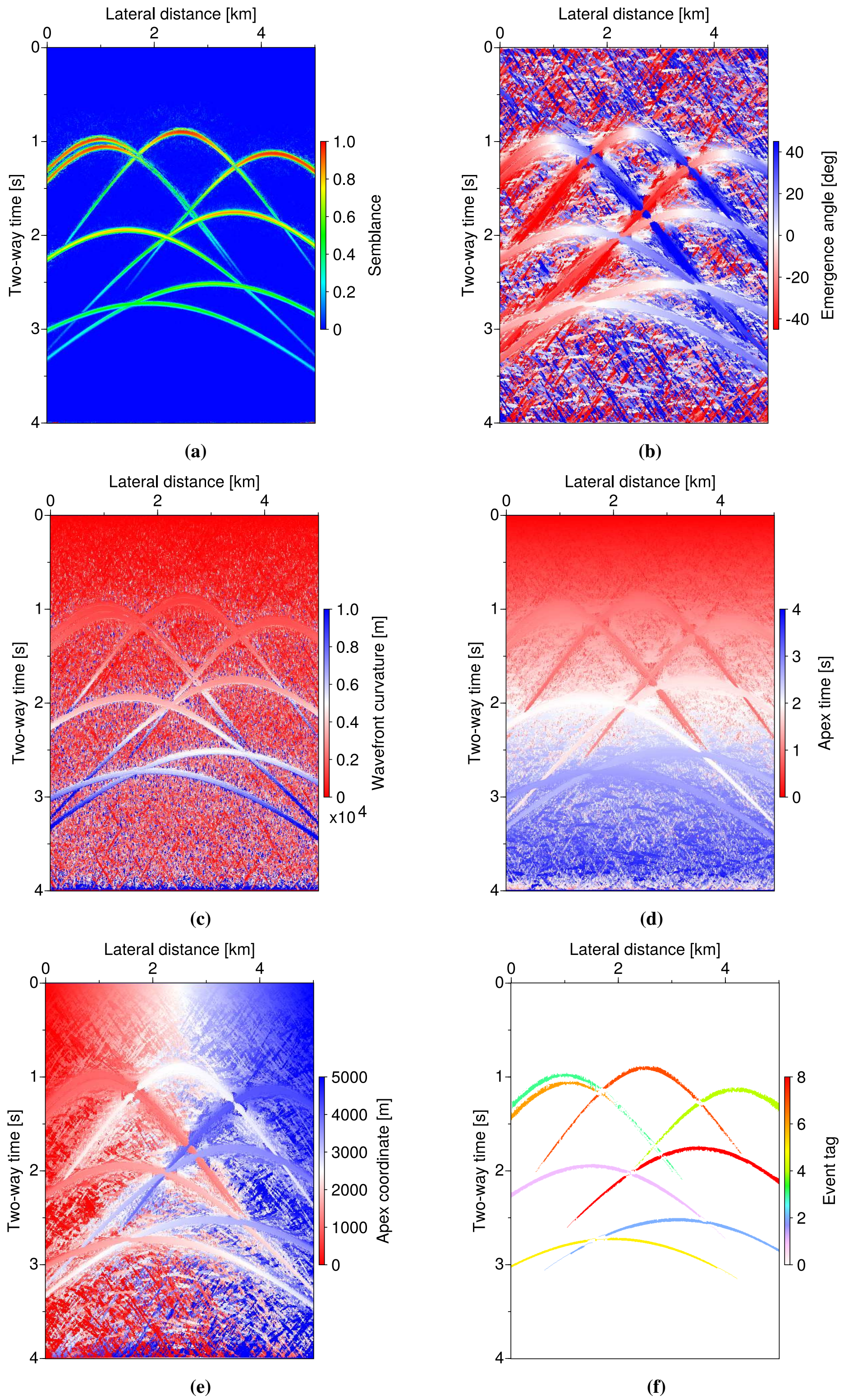

Figure 1: Synthetic diffraction example: (a) the zero-offset semblance, (b) the emergence angle α, (c) the wavefront curvature R_{NIP}, the apex coordinates (d) t_{apex} and (e) x_{apex} and (f) the resulting event tags.

AUTOMATIC TAGGING OF DIFFRACTIONS

The zero-offset wavefront attributes (Hubral, 1983) are physically meaningful parameters that are encoded in an events moveout and can be related to the first and second derivatives of the traveltime. A seismic reflection in 2D is characterized by three wavefront attributes: two wavefront curvatures, R_{NIP} and R_N, which describe two hypothetical waves excited by a point source placed on the normal-incidence point and an exploding reflector segment around the NIP, respectively, and their emergence angle at the recording surface α. In the case of a diffraction, however, the wavefront curvatures R_N and R_{NIP} coincide and thus, the number of wavefront attributes reduces to two. Furthermore, the remaining curvature R_{NIP} no longer describes a hypothetical wavefront, but the actually measured wavefront of the diffraction. The hyperbolic traveltime moveout for a diffraction is given by (Jäger et al., 2001)

$$\Delta t(t_0, x_0) = \sqrt{\left(t_0 + \frac{2\sin\alpha}{v_0}\Delta x_m\right)^2 + \frac{2t_0\cos^2\alpha}{v_0 R_{NIP}}(\Delta x_m^2 + h^2)} - t_0, \tag{1}$$

where h is the half-offset, Δx_m is the displacement from the central midpoint x_0, t_0 the reference traveltime, and v_0 the near-surface velocity. In 3D, the concept of the wavefront attributes is the same, but their number increases to five in the diffraction case and eight in the reflection case: two emergence angles and three or six wavefront curvatures, respectively. The attributes α and R_{NIP} can be transformed into apex coordinates (Mann, 2002) via

$$x_{apex}(x_0, t_0) = x_0 - \frac{R_{NIP} t_0 v_0 \sin\alpha}{2R_{NIP}\sin^2\alpha + t_0 v_0 \cos^2\alpha}, \qquad t_{apex}^2(x_0, t_0) = \frac{t_0^3 v_0 \cos^2\alpha}{2R_{NIP}\sin^2\alpha + t_0 v_0\cos^2\alpha}. \tag{2}$$

While these apex coordinates were initially designed for time migration, we use them as an additional criterion for our approach, since they are almost constant along a diffraction event.

For the global identification of events we assume that the wavefront attributes do not change abruptly along an event, i.e., that their local similarity is high although they vary globally. Since individual events are smooth no matter how strong the heterogeneity this assumption is reasonable. The first step is the detection of *valid* events, which is carried out trace-wise. For each sample with a coherence larger than a pre-defined threshold, we calculate the local similarity of the corresponding wavefront attributes within a window of n samples both above and below the considered sample i. The local similarity S_ϕ of a given attribute ϕ is the semblance coefficient (Neidell and Taner, 1971) given by

$$S_\phi(i,j) = \frac{1}{2n+1}\frac{\left(\sum_{k=i-n}^{i+n}\phi(k,j)\right)^2}{\sum_{k=i-n}^{i+n}\phi(k,j)^2}, \tag{3}$$

where j is the current trace. If the local similarity of all attributes (α, R_{NIP}, t_{apex}, and x_{apex}) is close to 1, the event is *valid* and a tag is assigned to it. If the previous n samples of the trace already contain an event tag, the corresponding wavefront attributes are compared directly by calculating their similarity via equation (3). If this similarity is close to 1 for all attributes, the event tag is copied. Otherwise, a new event tag is assigned to the current event. Next, we calculate the similarity of the assigned event tags S_{tags} for all traces.

After the detection of events on all traces, the contributions belonging to the same diffraction have to be matched laterally. For that, we define an additional window in midpoint direction, i.e. the maximum number of neighboring traces to be considered for the search of matching events. At each previously identified event, i.e. at each local maximum of S_{tags}, we calculate the local moveout of the event via equation (1). Then we step one trace to the left while shifting the search window into the direction of the event's moveout. In the resulting window we search for valid events and, for each found event, calculate the similarity of the corresponding wavefront attributes. If a matching event is found, the search is stopped and the event tag is copied to the respective sample. Otherwise, a new event tag is assigned to the sample under consideration. In order to remove outliers, we sort out tags with very few occurrences in the end. The proposed algorithm has also been implemented in 3D. However, in 3D the apex coordinates are not yet considered and instead of using the semblance coefficient for the calculation of the attribute similarity, the attributes are compared directly in the current implementation.

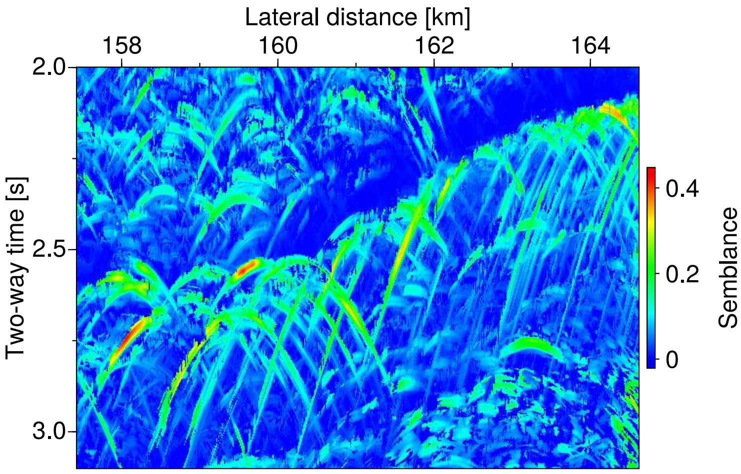

(a)

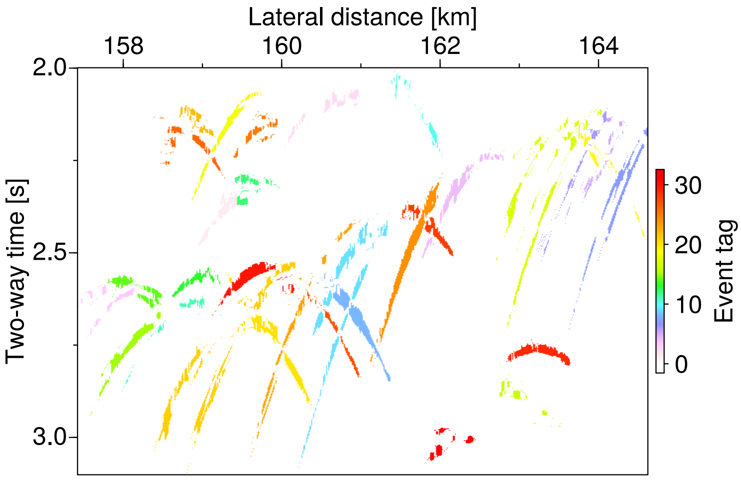

(b)

Figure 2: An excerpt of a field dataset from the Eastern Mediterranean: (a) the coherence after diffraction separation, and (b) the tags assigned to the diffractions.

DATA EXAMPLES

Figure 1 shows the input and the result of our proposed approach for a simple synthetic diffraction dataset, which contains eight diffractions in a vertically inhomogeneous medium and Gaussian noise with a S/N of 5. In the upper line, the results of the zero-offset CRS stack are displayed: the semblance section, the emergence angle α and the wavefront curvature R_{NIP}. Figures 1(d) and 1(e) show the apex coordinates calculated via equations (2). The resulting event tags are displayed in Figure 1(f). The result shows that all eight diffractions could be identified by assigning them a unique tag. The only problems occurred on the right branch of the two diffractions on the upper left side of the section, which could not be distinguished due to their vicinity.

Figure 2 shows the result of the event tagging for an excerpt of a field dataset from the Eastern Mediterranean, which contains a significant amount of diffracted energy. The diffraction coherence estimated after an attribute-driven diffraction separation (Dell and Gajewski, 2011) is displayed in Figure 2(a) and the resulting event tags in Figure 2(b). Due to the imperfect diffraction separation apparent in the coherence section, not all diffractions could be identified completely. However, the result shows that the majority of the coherently imaged diffractions could be individually identified with unique tags.

Figure 3 shows two crosslines of a simple synthetic 3D diffraction dataset similar to the one presented

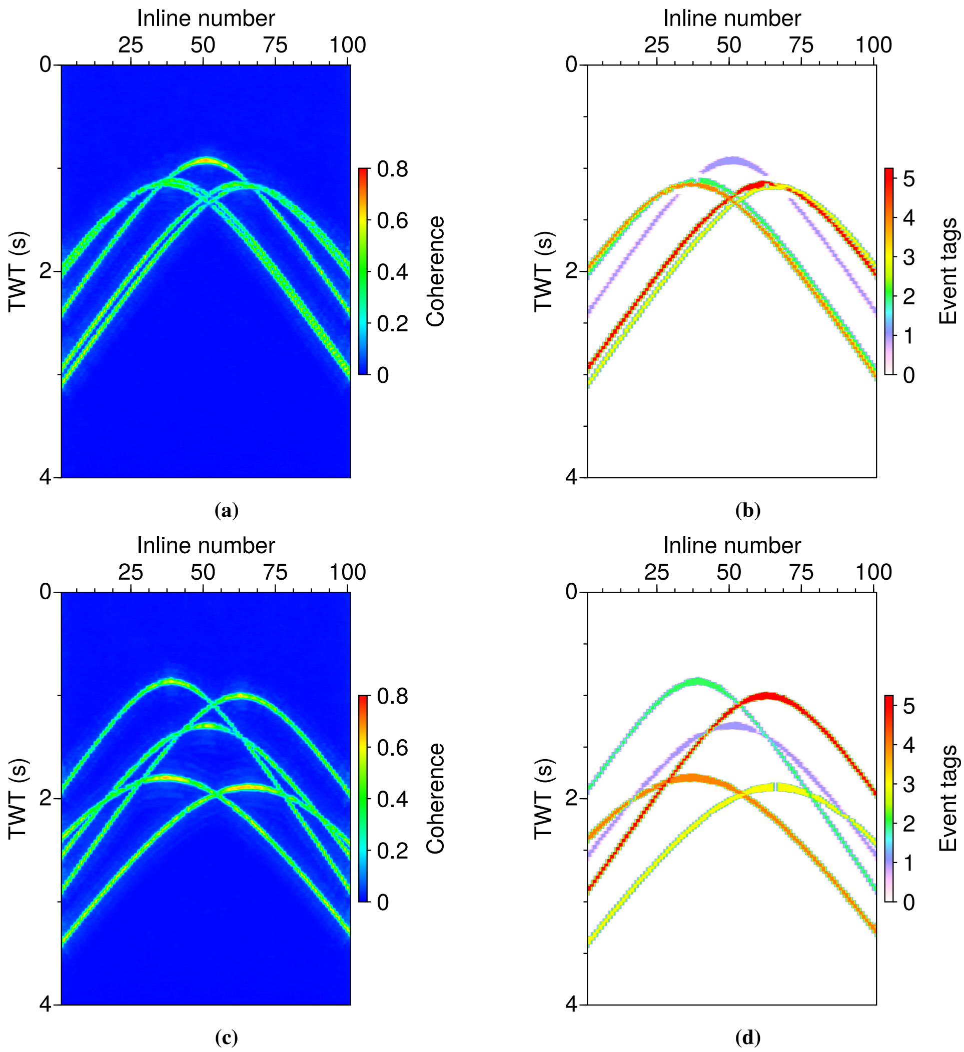

Figure 3: Two crosslines of the globally identified diffractions for a synthetic 3D diffraction dataset. The left sides (a,c) show the coherence obtained from the 3D CRS stack and the right sides (b,d) show the automatically assigned event tags.

in 2D. The left sides of Figure 3 show the semblance sections obtained from the CRS stack and the right sides show the corresponding event tags. The results reveal that all five diffractions could be identified and were assigned a unique tag. Even the two diffractions lying close to each other in Figure 3(b) could be distinguished due to the larger number of wavefront attributes available in 3D, which better constrain the problem.

CONCLUSIONS

We have presented a fully unsupervised scheme, which permits the detection diffractions based on their local coherence and analyzes the local similarity of their wavefront attributes to globally identify and tag common contributions. Results for 2D and 3D synthetic diffraction data and for a complex 2D field dataset suggest that the assumption of local attribute similarity is valid and that diffractions can be identified successfully even in complex settings due to the stability of the wavefront attributes. The global identification of diffractions paves the way for a better constrained wavefront tomography for diffractions and passive seismic data and for the assessment of uncertainties of velocity and localization.

ACKNOWLEDGMENTS

This work was supported by the Federal Ministry for Economic Affairs and Energy of Germany (BMWi, 03SX427B) and by the sponsors of the Wave Inversion Technology (WIT) consortium, Hamburg, Germany. We thank TGS for providing the field data. B. Schwarz is supported by a research fellowship of the German Research Foundation (DFG, SCHW 1870/1-1).

REFERENCES

Bauer, A., Schwarz, B., and Gajewski, D. (2016). Enhancement of prestack diffraction data and attributes using a traveltime decomposition approach. *Studia Geophysica et Geodaetica*, 60(3):471–486.

Bauer, A., Schwarz, B., and Gajewski, D. (2017a). Quantifying diffracted and passive event location uncertainties with local wavefront measurements. In *79th EAGE Conference and Exhibition 2017*.

Bauer, A., Schwarz, B., and Gajewski, D. (2017b). Utilizing diffractions in wavefront tomography. *Geophysics*, 82(2):R65–R73.

Baykulov, M. and Gajewski, D. (2009). Prestack seismic data enhancement with partial common-reflection-surface (CRS) stack. *Geophysics*, 74(3):V49–V58.

Dell, S. and Gajewski, D. (2011). Common-reflection-surface-based workflow for diffraction imaging. *Geophysics*, 76(5):S187–S195.

Diekmann, L., Schwarz, B., Bauer, A., and Gajewski, D. (2017). Approaching passive data with the established active seismic toolbox. In *79th EAGE Conference and Exhibition 2017 - Workshops*.

Duveneck, E. (2004). Velocity model estimation with data-derived wavefront attributes. *Geophysics*, 69(1):265–274.

Hubral, P. (1983). Computing true amplitude reflections in a laterally inhomogeneous earth. *Geophysics*, 48:1051–1062.

Jäger, R., Mann, J., Höcht, G., and Hubral, P. (2001). Common-reflection-surface stack: Image and attributes. *Geophysics*, 66:97–109.

Mann, J. (2002). *Extensions and applications of the common-reflection-surface stack method*. PhD thesis, University of Karlsruhe.

Neidell, N. S. and Taner, M. T. (1971). Semblance and other coherency measures for multichannel data. *Geophysics*, 36(3):482–497.

Schwarz, B., Bauer, A., and Gajewski, D. (2016). Passive seismic source localization via common-reflection-surface attributes. *Studia Geophysica et Geodaetica*, 60(3):531–546.

Schwarz, B. and Gajewski, D. (2017). Accessing the diffracted wavefield by coherent subtraction. *Geophysical Journal International*, 211(1):45–49.